

# Oscillating Water Column Wave Energy Converter for Low Wave Height Conditions

Geetam Saha\*<sup>‡</sup>, Dipesh Majumdar\*, Narasimalu Srikanth\*\*

\* Department of Construction Engineering, Faculty of Engineering & Technology, Jadavpur University, Kolkata, India

\*\* Energy Research Institute, Nanyang Technological University, Singapore

(sahageetam@gmail.com, dipeshce@jadavpuruniversity.in, nsrikanth@ntu.edu.sg)

<sup>‡</sup> Corresponding Author; Geetam Saha, Department of Construction Engineering, Faculty of Engineering & Technology, Jadavpur University, Kolkata, West Bengal, India, 700032, sahaageetam@gmail.com

*Received: 16.07.2021 Accepted: 19.08.2021*

**Abstract-** For continuous and uninterrupted energy extraction from marine wave motion, most of the existing wave energy extraction systems employ bi-directional turbines. The aerodynamic loss due to the symmetric placement of guide vanes results in a major power output reduction in the system. To optimize this problem, researchers have developed and tested a variety of oscillating water column air turbines. Most commonly used are the axial turbines because of their simplicity and operational ease. The present work focuses on a novel design of an oscillating water column energy extraction system based on a unidirectional axial impulse turbine with a novel rectifying system arrangement which primarily focuses to minimize the losses due to downstream guide vanes and in turn shoot up the power output for low wave height conditions. A numerical model was developed and investigated using RANS equations and  $k-\omega$  SST turbulence model. The obtained results portray that the proposed flap-based bi-directional impulse system is operationally viable and produces substantially greater power output in comparison to conventional bi-directional and uni-directional turbine systems under low wave height conditions. A hybrid choking scheme was followed which resulted in additional power output. Results show that full choking of the idle turbine is ensured during the inhalation cycle, which was not possible earlier. During the exhalation cycle, additional power output was also obtained from the secondary turbine i.e., front end turbine during exhalation cycle. The proposed system generates maximum total power output at around a flow coefficient of 1.

**Keywords** Computational Fluid Dynamics; Renewable; Oscillating Water Column; Wave Energy; Low Wave Height

## 1. Introduction

The oscillating water column (OWC) wave energy converters (WEC) are the most extensively used devices across the world for ocean wave energy harvesting. The primary design requirement in such systems is continuous energy extraction during inhalation as well as exhalation in the phylum/air chamber of OWC WEC irrespective of the direction of oscillating water flow. Conventional uni-directional flow turbines with non-return valves are an option for this purpose [1]. Rectifying valve systems were successfully used in navigation buoys.

But these were impractical in large plants, where flow rates are in order of  $100 \text{ m}^3\text{s}^{-1}$  and the required response time is typically less than 1s [2]. To resolve this problem, a new class of turbines came up which were known as self-rectifying bi-directional turbines. Most of the self-rectifying air turbines used for wave energy conversion are in axial-flow configuration. They are of two basic types: Well's

turbine and impulse turbine. In 1976, Well's turbine was invented by Dr. Alan A. Wells [3]. The first patent for self-rectifying impulse turbine was granted to I. A. Babinstevev in 1975 [4]. Fig. 1 presents the comparison of various types of self-rectifying turbines with uni-directional turbines. It is clearly visible from Fig. 1 that uni-directional turbines are highly efficient in comparison to bi-directional turbines for wave energy extraction, resulting in higher power outputs. The present work focuses on the development of a WEC for low wave height conditions.

The efficiency of an OWC WEC system depends on the individual efficiencies of 3 components. They are the OWC chamber, turbine and generator. Fundamentally, OWC WEC is based on the utilization of the dynamic air movements and associated pneumatic pressure from the ocean wave motion of the OWC.

In low wave height conditions, pneumatic pressure due to wave motion is limited in comparison to moderate or extreme wave height conditions.

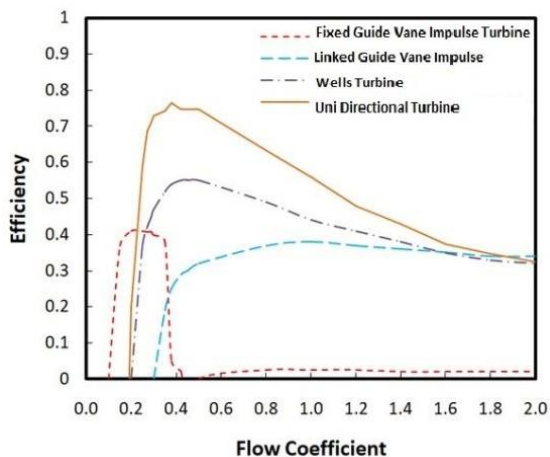


Fig. 1. Comparison of different classes of turbines [5-7]

It is clear from this fact that conventional design won't work be optimal in such conditions. The study of global wave energy from reanalysis and hindcast data done by Arinaga and Cheung provides the percentile plots of significant wave heights across the world and reveals the fact that Indian wave height conditions are relatively low with significant wave heights less than 2 m for 70% of the time [8]. South Asian countries such as India, Myanmar, Vietnam, Cambodia, Thailand have considerably lower wave heights in comparison to European and American nations, where ocean wave energy is harnessed widely.

The conventionally used self-rectifying Wells and impulse turbines face a major aerodynamic loss due the symmetry of guide vanes which results in lower power output. In low wave height conditions, the results will be worst. Because of this particular problem, requirement specific design is essential. In this regard, flap-based fixed type OWC WEC is designed and investigated specifically for low wave height conditions in the present study.

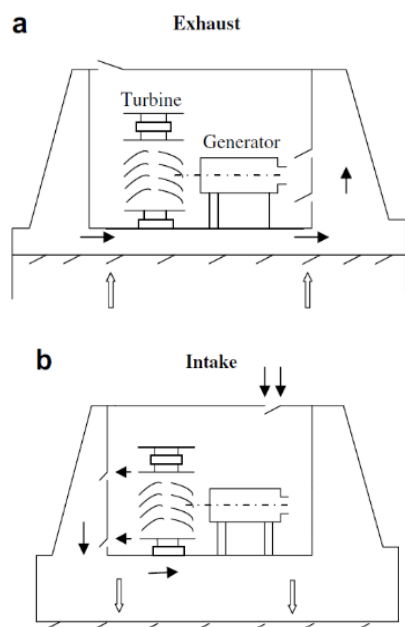


Fig. 2. Typical OWC plant with UDI turbine [35]

## 2. Background

Development in science and technology has led to a spontaneous increase in energy demand but resources are limited. To cope up with the energy crisis, majority of the nations are struggling to assimilate new energy alternatives into the mainstream power grid. Due to the rapid continuous utilization of conventional energy sources and their resultant environmental impact, researchers are compelled to look for alternative energy resources which could replace them [9]. As per the current environmental scenario in urban localities across the world, one of the mandatory requisites for the alternative is minimal or no environmental impact. Another important parameter is that the alternative must be non-exhaustible and sustainable. Marine energy can act as an excellent alternative. Intense research work has been in progress since the last decade specifically focusing on marine wave and wind energy [10-15]. OWC technology has been employed for a long time in ocean wave energy harvesting systems. For energy extraction from incoming as well as outgoing waves, bi-directional turbines are utilized. Bi-directional turbines of both types, impulse and reaction use downstream guide vanes (DGV) for continuous energy harvesting.

For increasing the efficiency of the bi-directional turbines, a series of inventions have been done by researchers based on various optimization approaches [16-34]. Major developments include optimized design of aerofoil of rotor blades and development of various types of guide vanes such as self-pitch controlled and active pitch control. But despite all these developments, an inherited fallacy of self-rectifying bi-directional turbines is the major loss in power output due to the presence of guide vanes in the downstream direction still continues to exist. It is apparent that a need exists for a technique or technology where this considerable loss can be minimized. The present work is directed towards providing such a technique. The main objective of the present work is to provide a method and a system where the power output drops of the wave energy converter due to downstream guide

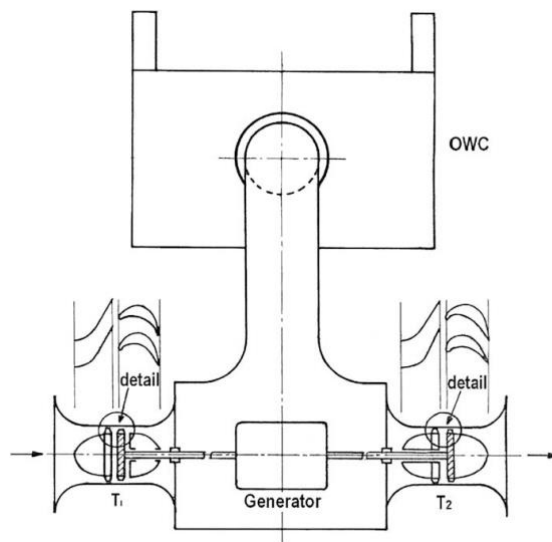


Fig. 3. Twin UDI turbine topology [35]

vanes in bi-directional turbine WECs can be minimized under low wave height conditions.

Fig. 2 presents the typical conventional OWC WECs employing unidirectional turbine with rectifying system for wave energy extraction. As depicted by Fig. 2, two types of valves are used during air intake. Similarly, during exhaust two types of valves are used. In total, for the complete operation of the system, four types of valves are necessary. For extraction of wave power with unidirectional turbines, Jayashankar et. al. developed a twin uni-directional turbine topology. Fig. 3 depicts the schematic diagram of the twin topology system. The results obtained from the system portrayed that even though full choking is not possible in the reverse direction but performance is still appreciable [35]. Okuhara et. al. performed further analysis on a similar experimental setup and suggested some optimizations regarding guide vane solidity [36].

**3. Proposed System: Flap based Oscillating Water Column Wave Energy Converter**

The proposed system consists of a flap-based ocean wave energy converter comprising dual rotors. Generally, wave energy converters consist of bi-directional turbines which have guide vanes on both sides of rotor blades. The present work focuses on the design of an ocean wave energy converter that utilizes energy from both incoming and outgoing waves but without using downstream guide vanes. Instead, it is made possible to harness wave energy in a continuous and uninterrupted way with enhanced power output by employing dual rotors with single guide vanes which work in two half cycles. This is done by implementing an operational cycle that uses axial and sidewall flaps to work in a synchronized way with the direction of airflow and movement of the oscillating water column. The operational

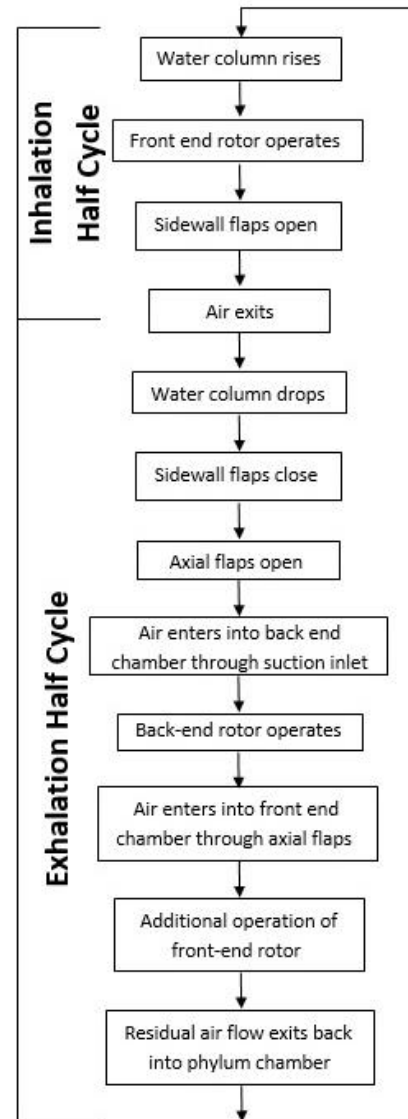


Fig. 4. Working Methodology

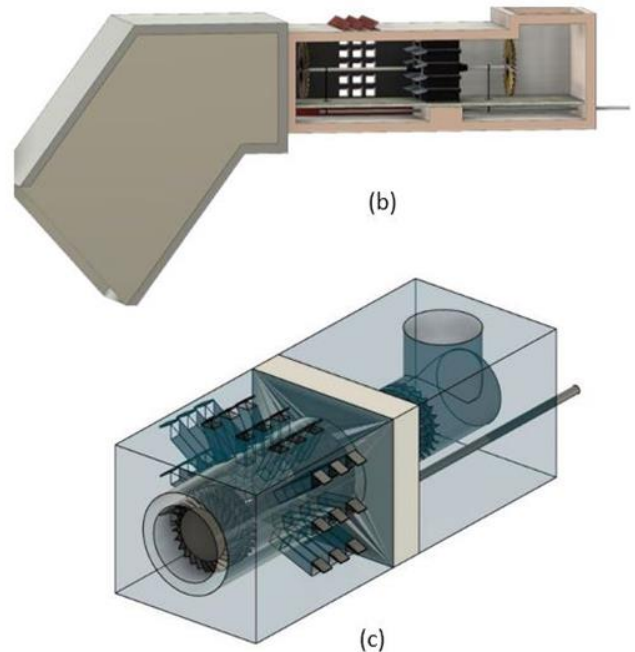
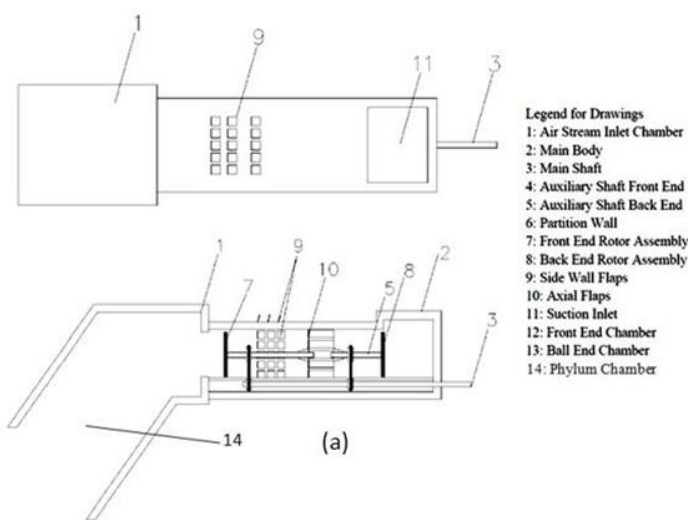


Fig. 5. Proposed Model: (a) Plan & Section (b) 3D Model (c) Simplified Model

cycle runs in two synchronized half cycles. The schematic diagram and conceptual 3D drawings are shown in Fig. 5 (a &b) respectively. The 3D model used for numerical investigation is shown in Fig. 5(c).

During the first half cycle, power take-off is due to the incoming wave motion or upstream motion of the water column. This upstream motion causes wave-induced air pressurization in the air capture chamber or phylum chamber of the OWC. As a result, the sidewall flaps open. Due to this increase in air pressure, a pressure gradient is generated and an airstream moves through the front-end chamber. As a result of this movement, the front-end rotor assembly operates and the power take-off mechanism transmits the power to the main shaft through the front-end auxiliary shaft.

In the second half cycle, power take-off is due to outgoing waves or downstream motion of the water column. This downstream motion causes a suction effect in the airstream inlet chamber which is transmitted to the main body. This causes axial flaps to open and sidewall flaps to close. Due to this drop in pressure, a pressure gradient is generated and air stream enters through the suction inlet and moves through the back-end chamber. Due to this movement, the back-end rotor assembly is driven and the power take-off mechanism transmits power to the main shaft through the back-end auxiliary shaft. These two half-cycles continue to operate one after another resulting in an uninterrupted and continuous power supply with an increased power output in comparison to self-rectifying bi-directional turbine-based oscillating water column wave energy converters. The entire work methodology is shown in Fig. 4. As mentioned in Fig. 4 there is additional power output from the front-end rotor during the exhalation cycle. This provision is discussed in section 5 along with the simulation results.

**4. Numerical Study**

In the present work, a novel system is proposed. For investigation of its reliability and performance, a numerical study was performed. The study was performed via 2 approaches, contemporary and holistic. The contemporary approach was considered to perform a comparative analysis of UDI and BDI turbines. As in the present work UDI turbine is utilized so it was investigated under both inhalation and exhalation work cycles.

The single set of RB and GV was analysed under the contemporary approach for the UDI turbine was in turn used for the generation of entire 3D geometry of the turbine. The generated turbine geometry was investigated inside the simplified model of the proposed flap-based system under a holistic approach. The numerical study was performed using commercial code CFX.

*4.1. Contemporary Approach*

The numerical study under this approach focuses on performance analysis of the turbine by investigating a set of a rotor blade, two guide vanes for BDI turbine. A set of rotor blade and a guide vane was considered for UDI turbine. Investigation of a single set results in a reduction of computational time and cost. The UDI turbine was simulated for both inhalation and exhalation cycles. The inhalation cycle stands for incoming wave motion and the exhalation cycle stands for outgoing wave motion.

**Table 1:** Rotor Blade and Guide Vane Profile Details

Design Parameter	Specification
$X_{ss}$	125.8
$Y_{ss}$	41.4
$R_{ps}$	30.2
$l_{rb}$	54
$L_{gv}$	34.8
$R_{gv}$	37.2
$L_{gv}$	70
$\rho_{rb}$	0.5
$\theta$	60°
$\delta$	30°
$\lambda$	20
$\rho_{gv}$	0.5
$\sigma$	1
$v$	16.1

*4.1.1. Turbine Specifications & Reference Geometry*

The reference geometry for the present work was taken from [24]. This geometry was first used by Maeda et.al. in 1998 for experimental purposes and has been predominantly in use for bi-directional self-rectifying turbines till date. The turbine consists of 30 rotor blades and 26 guide vanes. The turbine has a hub and tip

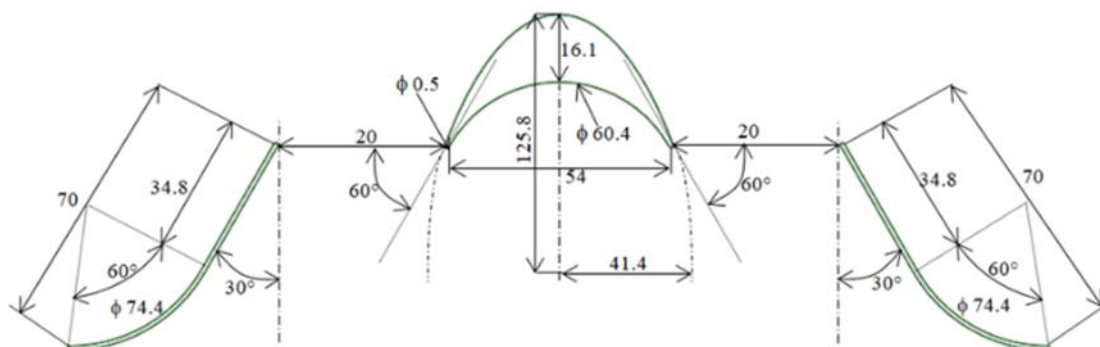


**Fig. 6:** RB and GV Profile

diameter of 210 and 298 mm respectively. Tip clearance of 1 mm is present between blade and shroud.

4.1.2. Numerical Methodology

The numerical analysis for the present work was performed by using commercial code ANSYS CFX which uses Navier-Stokes equations for the conversions of mass and momentum was used for solving the problem. The governing Navier-Stokes’s transport equations are as given by Equations 1 to 4.

$$\frac{\partial(\rho u)}{\partial x} + \frac{\partial(\rho v)}{\partial y} + \frac{\partial(\rho w)}{\partial z} = 0 \quad (1)$$

$$-\frac{\partial(P)}{\partial x} + \frac{\partial(\tau_{xx})}{\partial x} + \frac{\partial(\tau_{yx})}{\partial y} + \frac{\partial(\tau_{zx})}{\partial z} = \text{div}(\rho_{uu}) \quad (2)$$

$$-\frac{\partial(P)}{\partial x} + \frac{\partial(\tau_{xy})}{\partial x} + \frac{\partial(\tau_{yy})}{\partial y} + \frac{\partial(\tau_{zy})}{\partial z} = \text{div}(\rho_{vu}) \quad (3)$$

$$-\frac{\partial(P)}{\partial x} + \frac{\partial(\tau_{xz})}{\partial x} + \frac{\partial(\tau_{yz})}{\partial y} + \frac{\partial(\tau_{zz})}{\partial z} = \text{div}(\rho_{wu}) \quad (4)$$

The computational domain has been divided into 3 sub domains. Upstream Guide Vane (UGV), Rotor Blade (RB), Downstream Guide Vane (DGV) domains. The UGV and DGV domains are stationary domains whereas RB domain is rotating at 700 rpm.

One major complexity of numerical simulation of this particular problem is the different rotational speeds of individual cell zones. Hence, in this present work, multiple reference frame or the frozen rotor approach was adopted. At the interfaces between cell zones, a local reference frame transformation is performed to enable flow variables in one zone to be used to calculate fluxes at the boundary of the adjacent zone [37]. Based on the simulation conditions, the k- ω Shear Stress Transport turbulence model was used with 5% turbulence intensity.

Fig. 7 presents the computational domain and the boundary conditions for the steady-state numerical simulation of the BDI turbine. Rotational periodic boundary condition was applied on the UGV subdomain inlet. Nil

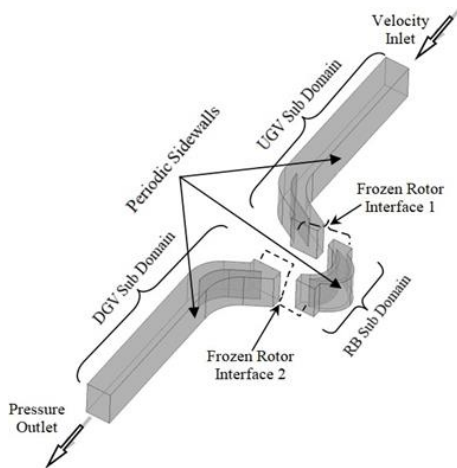


Fig. 7: BDI Computational Domain

relative pressure condition was imposed at DGV sub domain outlet. The convergence criteria chosen for the analysis was 1.0E-05.

Fig. 8 presents the computational domain and boundary conditions for the steady-state numerical simulation of the UDI turbine for the inhalation half cycle. Similar periodic boundary conditions were imposed in this case too as in the case of BDI. The same velocity inlet boundary condition as imposed in the previous case was applied here. In this case, nil relative pressure condition was imposed at the outlet of the rotor blade. Similar convergence criterion was used here too.

The final case under this approach was the steady-state numerical simulation of the UDI turbine for exhalation half cycle. Rotational periodic boundary conditions for sidewalls were imposed as done in the previous cases. Under exhalation cycle (outgoing wave motion), velocity inlet boundary condition was imposed at the end of the rotor blade with no guide vane. Nil relative pressure boundary condition was imposed at the inlet end of the guide vane. The convergence criteria chosen for the analysis was 1.0E-05.

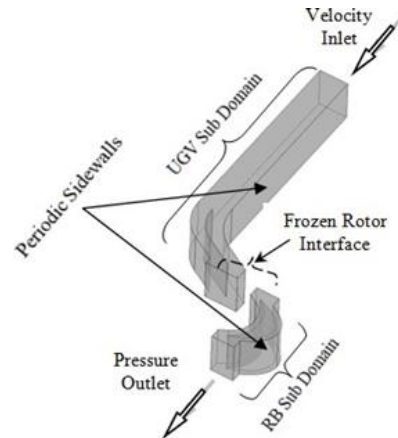


Fig. 8: UDI Computational Domain (Inhalation)

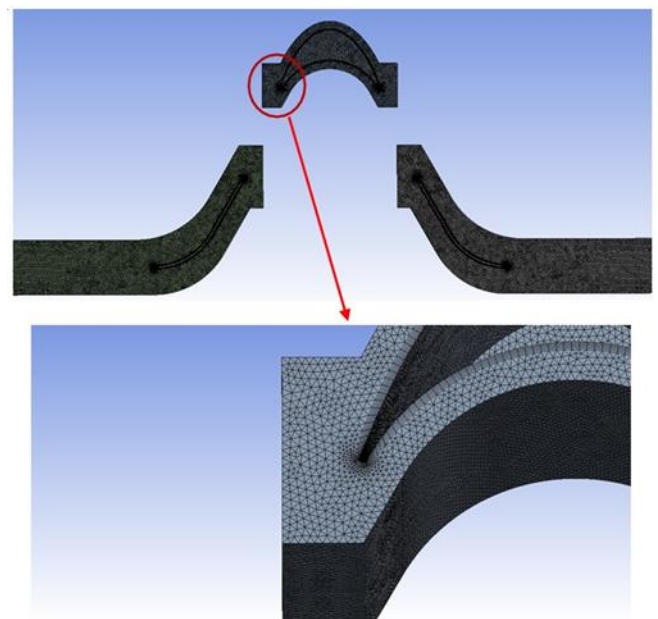


Fig. 9: Mesh

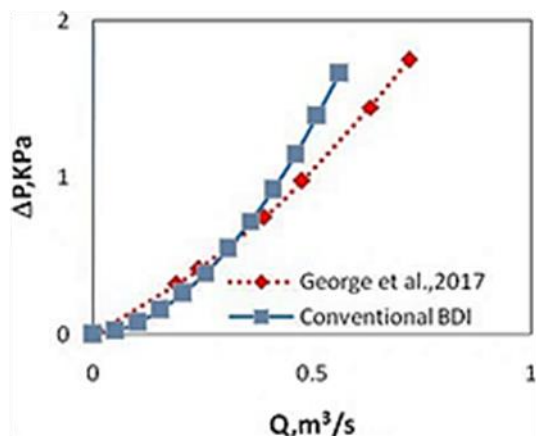


Fig. 10: Pressure Difference vs. Volume Flow Rate

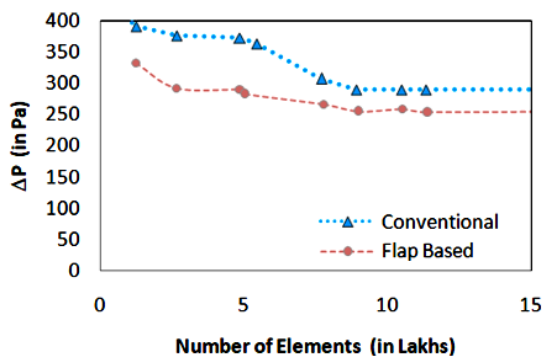


Fig. 11: (a) Grid Independence Test

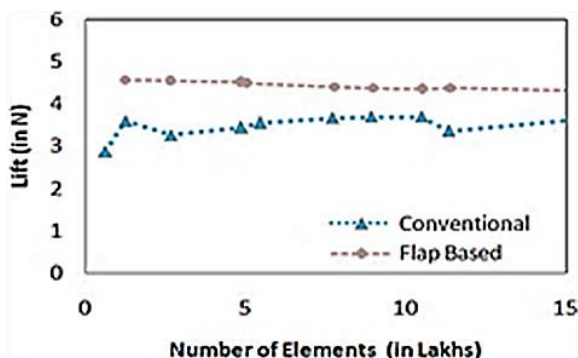


Fig. 11: (b) Grid Independence Test

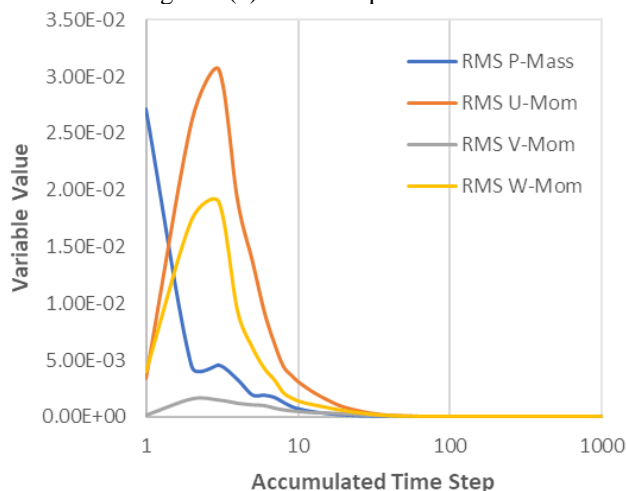


Fig. 11: (c) Residuals Plot

#### 4.1.3. Validation

The validation procedure was done for the conventional self-rectifying BDI turbine model with 30 rotor blades and 26 guide vanes. The grid independence was established for both conventional BDI and the proposed model. Grid independence was checked via eleven different mesh counts. Residual convergence was also established with the optimal grid size. Fig. 11 reveals that lift and converged after 1.485 million elements with a size of 0.005 m. Henceforth, 1.485 million mesh elements were taken for the study. In an analytical study by George et al. [18] the  $\Delta P$  vs.  $Q$  comparison was made for different diameters. The present study focuses specifically on 298mm BDI. A comparison of the present numerical study with the study by George et. al. as mentioned above is presented in Fig. 10. The difference with the data values is nearly in the range of 10%.

#### 4.2. Holistic Approach

In the present work, along with the investigation via a contemporary approach, a holistic approach to predict the functioning of the proposed model was performed. Under this approach, the typical model as shown in Fig. 5 was separated into two components, front end and back-end chamber for the study.

##### 4.2.1. Specifications

The simplified version of the 3D model shown in Fig. 5(c) was considered for numerical investigation. The fluid flow passage was modelled for both front-end and back-end chambers. As mentioned in section 4.1.1, the tip diameter of the turbine was considered as 298 mm with 1 mm tip clearance, hence the fluid flow domain has a diameter of 0.3 m. Lengths of the front end and back-end chamber computational domains were 700 mm and 600 mm respectively.

##### 4.2.2. Methodology

The back-end chamber of the proposed system is under operation only during the exhalation cycle as a result it was simulated only for the exhalation cycle. Whereas the front-end chamber was investigated for both inhalation as well as exhalation cycle. As a result, three operational cases were investigated under the holistic approach. Fig. 12 presents the computational domain for the back-end chamber for steady-state numerical analysis during the exhalation cycle.

Velocity inlet boundary condition was imposed at the suction inlet of the back-end chamber. Pressure outlet boundary condition was applied at the axial flap openings of the back-end chamber. Fig. 13 presents the computational domain of the front-end chamber for steady-state numerical investigation during the inhalation half cycle. For reduction in computational time, only a quarter of the front-end rotor was considered for numerical investigation. Rotational periodic boundary condition was utilized in this case. Velocity inlet boundary condition was used at the inlet end (from the phylum chamber) of the front-end chamber.

Pressure outlet boundary condition was used at sidewall flaps. Fig. 14 presents the computational domain of the front-end chamber for steady-state numerical investigation during the exhalation half cycle. Velocity inlet boundary condition was imposed at the axial flap openings. Pressure outlet

boundary condition was imposed at the inlet end (from the phylum chamber) of the front-end chamber along with side wall flaps. In all the three computational cases, the convergence criteria were chosen as 1.0E-04.

#### 4.2.3 Mesh

The fluid flow domain of the back-end chamber was investigated as a whole. The mesh count for the back-end chamber computational domain was approximately 28 million. Fig. 15 presents the same. Only a quarter of the front-end chamber was considered for numerical investigation. The mesh count for the front-end chamber computational domain was approximately 7 million. Fig. 16 presents the same.

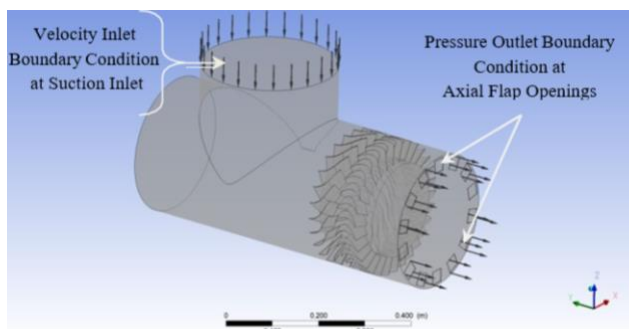


Fig. 12: Back End Chamber Computational Domain

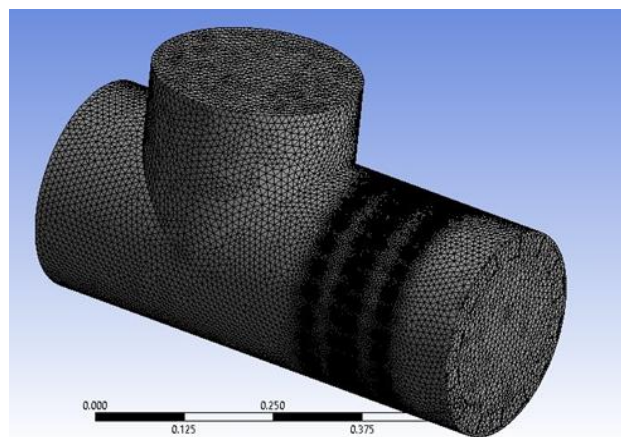


Fig. 15: Mesh (Back End Chamber)

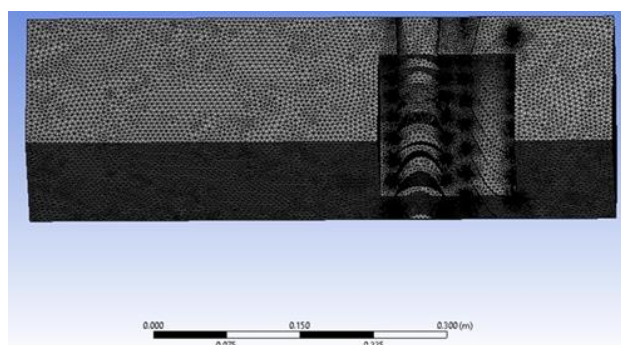


Fig. 16: Mesh (Front End Chamber)

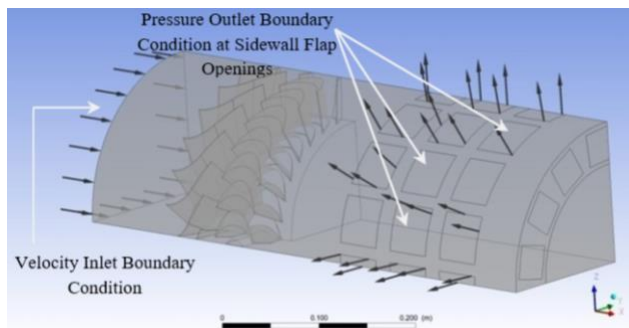


Fig. 13: Front End Chamber Computational Domain: Inhalation Cycle

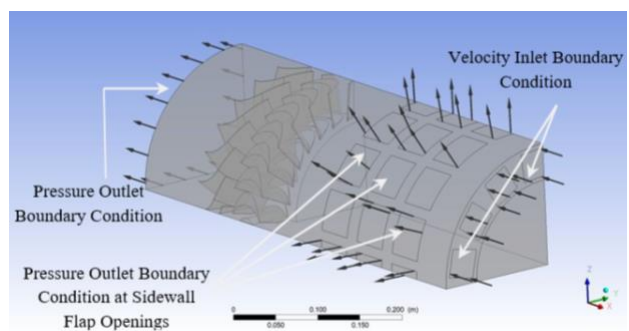


Fig. 14: Front End Chamber Computational Domain: Exhalation Cycle

## 5. Results and Discussion

The numerical study was performed under 3D flow conditions as per the methodologies described in sections 4.1.2 and 4.2.2. For the comparative analysis, conventional BDI turbine and the proposed UDI turbine were investigated at different operational cases i.e., inhalation and exhalation under flow coefficients ranging from 0.5 to 2.5. The flow coefficient is defined as the ratio between axial flow velocity and the blade peripheral velocity.

$$\Phi = V_a / U \quad (5)$$

In the present study, variation of flow coefficient is done by changing the axial flow velocity keeping the blade peripheral velocity constant. Fig. 17 presents the performance comparison of the conventional BDI and flap-based UDI turbine in terms of the lift produced on the rotor blade and the pressure drop across the turbine ( $\Delta P$ ) at different values of flow coefficient. The lift produced in case of the conventional BDI is less than the flap-based UDI in the flow coefficient range of 0.5 to 2.5. It will ultimately result in enhanced power output in comparison to conventional BDI turbines. It is also evident that maximum lift is produced at around flow coefficient 1.5. The pressure drops in case of flap-based UDI is considerably more in comparison to the conventional BDI turbines. Pressure drop across a turbine is an input characteristic that gives an idea about the energy input into the turbine. In case of performance evaluation of OWC turbine, power output is more reasonable than energy input because energy available from OWC or ocean is abundant and practically free of cost.

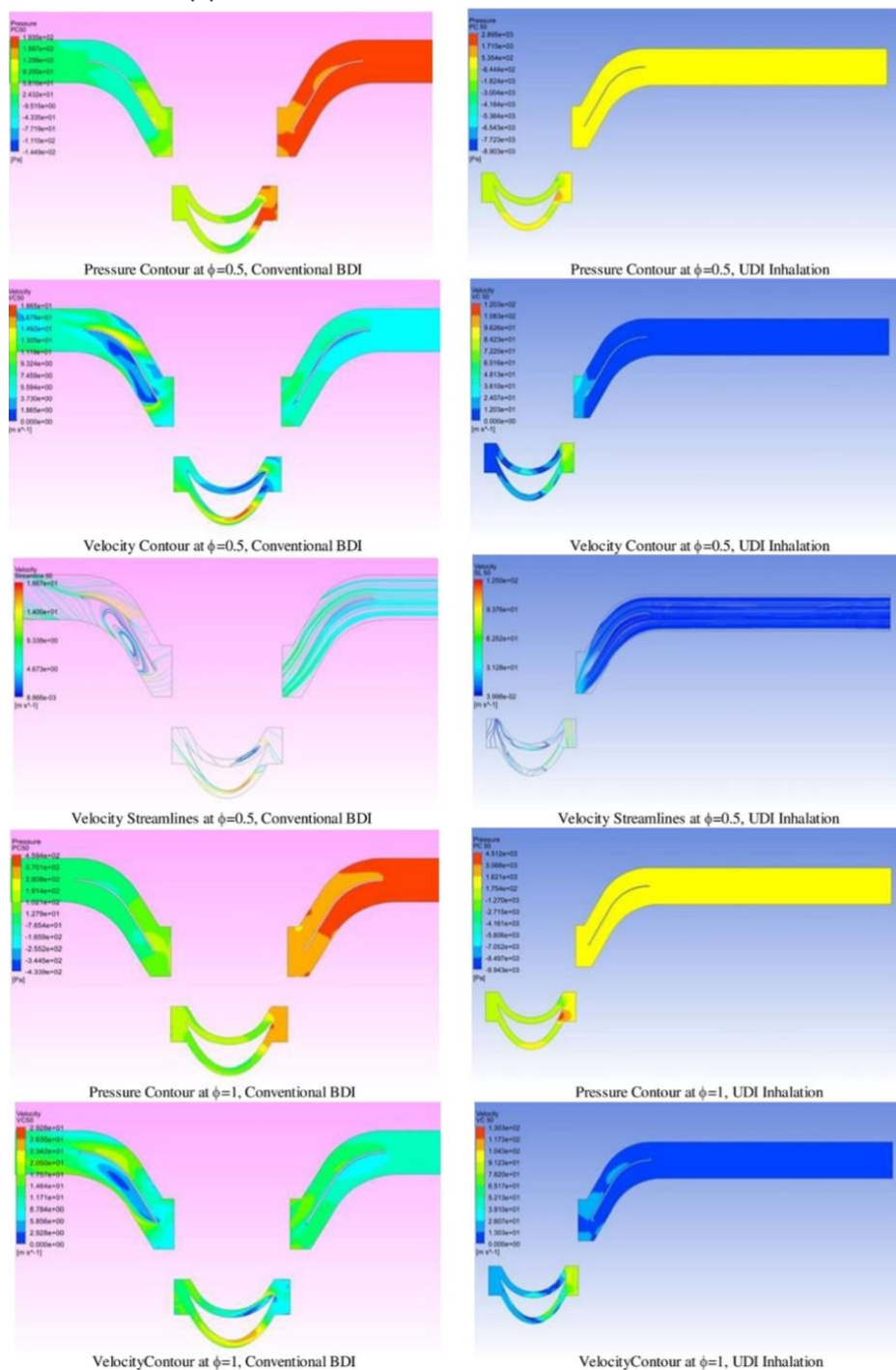
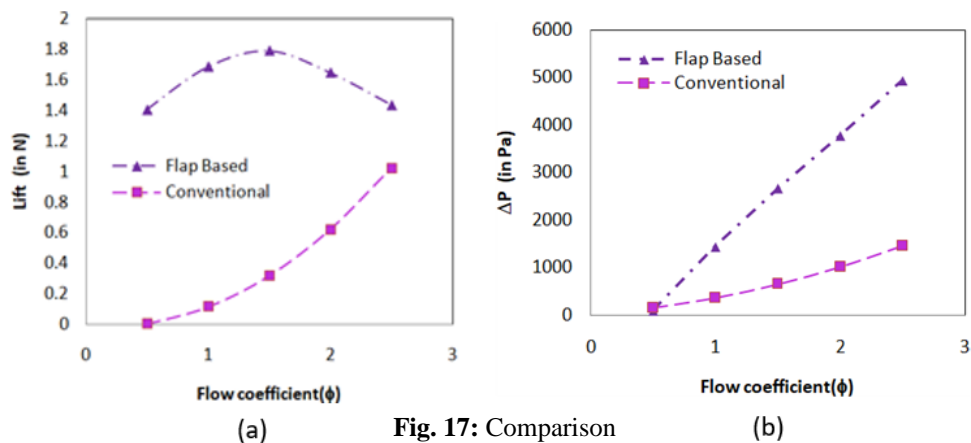
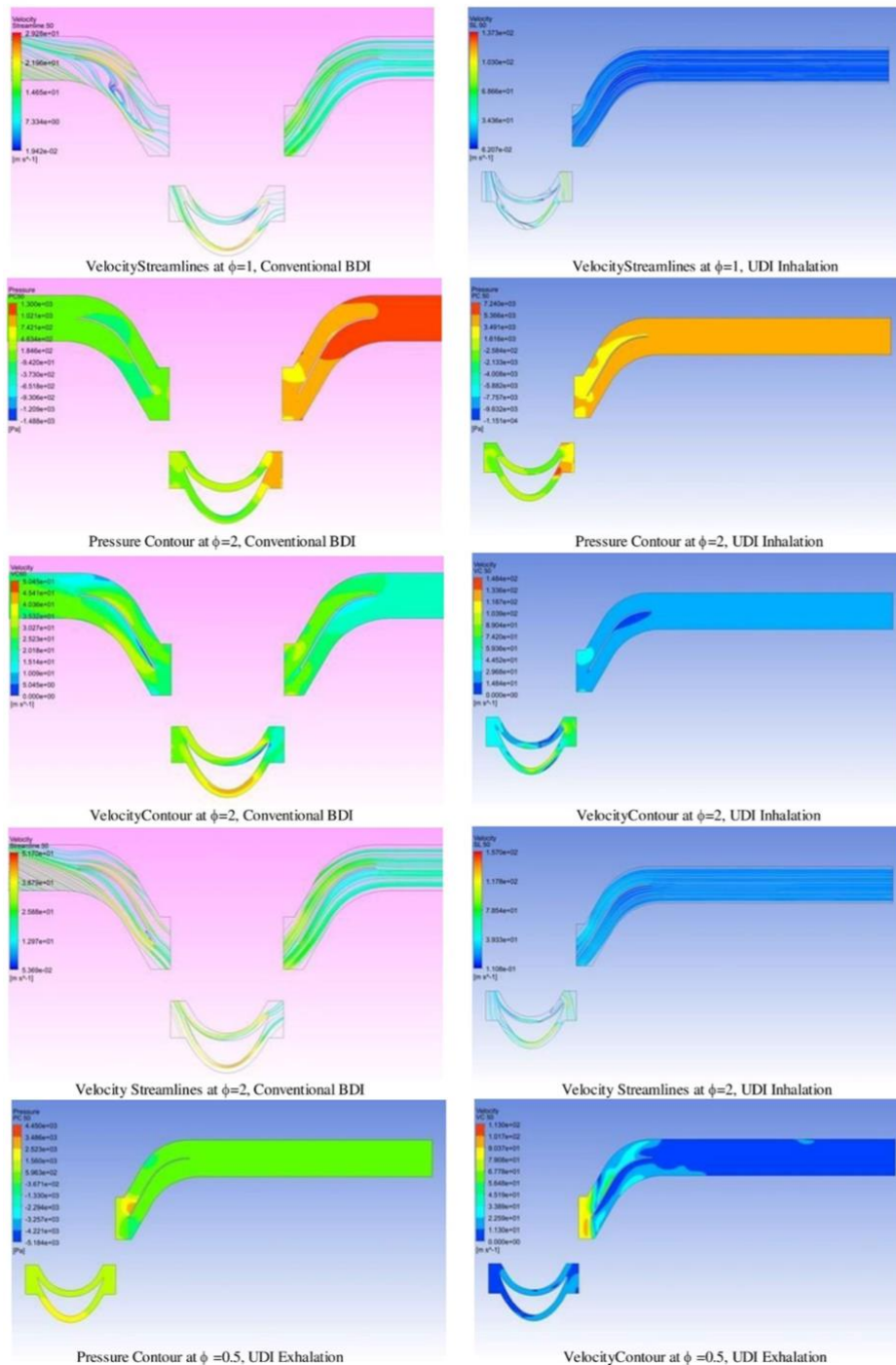


Fig. 18: Velocity & Pressure Contours, Surface Streamline



**Fig. 19:** Velocity & Pressure Contours, Surface Streamline

As the present work focuses upon low wave height conditions, consideration of power output for evaluation is more reasonable.

The pressure contours, velocity contours and velocity streamlines are presented for a plane passing through 50% blade height for the three operational cases (BDI, UDI inhalation and exhalation) under flow coefficients 0.5, 1, 2 in Fig. 18 to 20.

On comparing the velocity contours of the BDI and UDI under inhalation cycle as presented in Fig. 18 and 19. It is evident that the velocity drop across the rotor blade is substantially higher in UDI in comparison to BDI. From

Euler’s turbine equation, it is well known that the higher the velocity change or momentum transfer across the RB greater is the work done/power output [38]. This finding is also in line with Fig. 17(a). It can be commented from this observation that the UDI turbines produce higher power output in comparison to conventional BDI turbines for OWC applications.

The pressure contours of BDI and UDI under inhalation cycle as presented in Fig. 18 and 19 supports the finding that UDI has considerable pressure drop across the turbine in comparison to the conventional BDI turbine across the entire flow coefficient range under investigation (Fig. 17(b)). On comparing velocity streamlines of BDI and UDI Inhalation

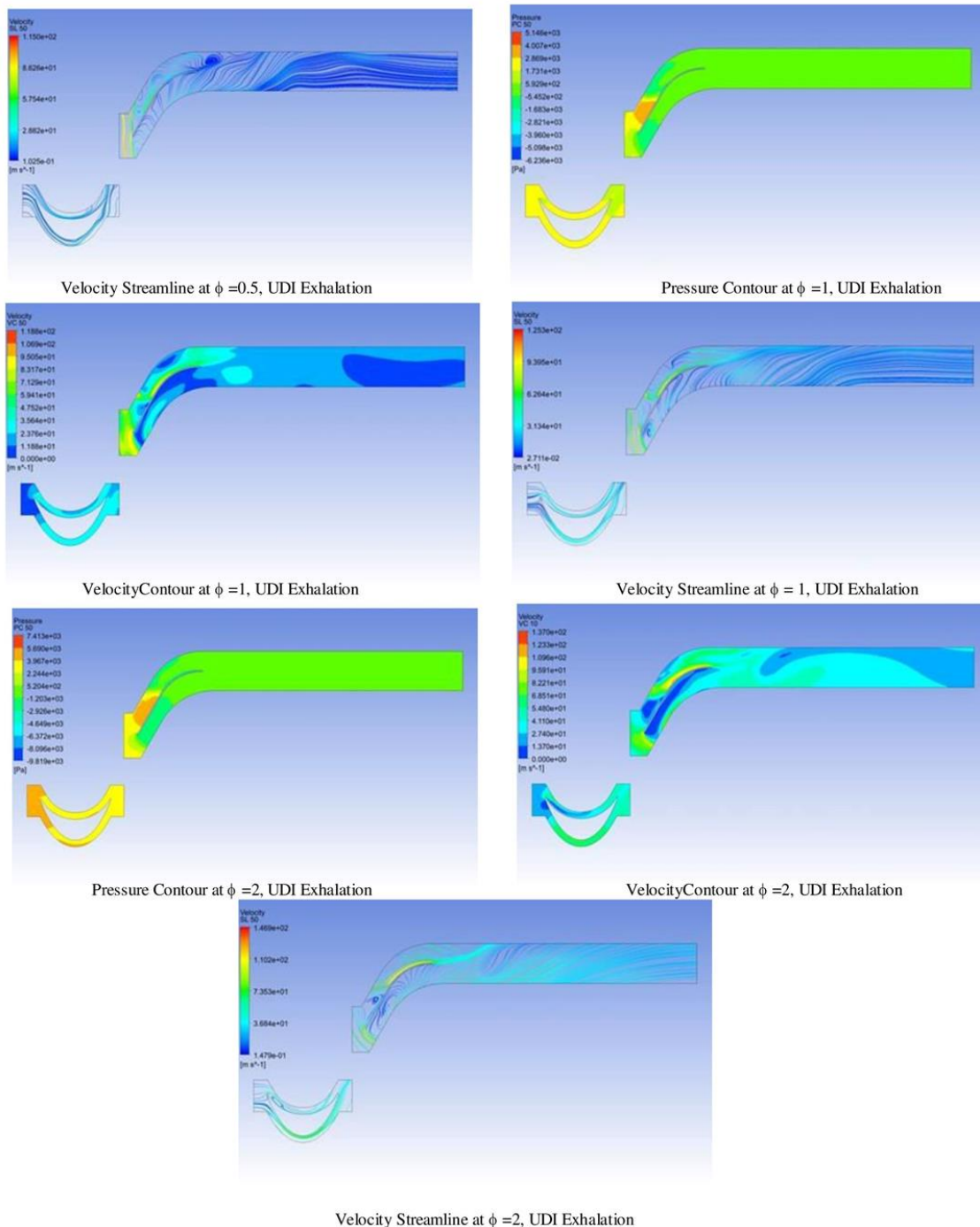


**Fig. 20:** Velocity & Pressure Contours, Surface Streamline

under flow coefficient of 0.5, it is evident that the fluid flow is uniform and similar in UGV of both BDI turbine and UDI turbine. But there is a fluid flow separation at the trailing edge of the rotor blade in BDI turbine in comparison to the UDI turbine. Contrary to the results of flow coefficient 0.5, on comparing velocity streamlines under flow coefficient 1, it is visible that the flow is attached to the RB trailing edge. But flow separation occurs at the leading edge of the BDI turbine. This flow separation at leading and trailing edge of the rotor blade of BDI seems to be a reason behind lesser momentum transfer from fluid(air) to the rotor blade which leads to reduced lift generation and less power output under lower coefficients like 0.5 and 1. On Comparing the velocity

streamlines at a high flow coefficient of 2, it is clearly visible that the flow is attached very well to the rotor blade in the BDI turbine but in the case of the UDI turbine, the flow separation appears near the trailing edge at the suction side of the rotor blade. This separation results in the reduced lift, which is conformant with results as shown in Fig. 17(a). Under the holistic approach, the fluid flow domains of the front and back-end chamber of the proposed flap-based system were investigated separately under different half cycles. The motive behind this was to investigate the operational reliability of the proposed system. The flow in both chambers was visualized by the generation of 3D streamlines in the computational domains.

Fig. 21 presents the fluid flow inside the back-end chamber during the exhalation cycle through 3D velocity streamlines. It is clearly visible that the majority of the fluid flow takes place directly from the suction inlet to the turbine assembly but a certain portion of the circulation of fluid flow takes place at the trailing end of the back-end chamber. The torque produced in the back-end rotor was comparable to results obtained in the contemporary approach. The vortices at the trailing end result in minor losses in power capture. These vortices can be reduced by shape optimization of the trailing end of the back-end chamber.

Fig. 22 presents the fluid flow inside the front-end chamber during the inhalation cycle through 3D velocity streamlines. It is evident that the fluid flow occurs fairly across the front-end rotor assembly and flow exits from side wall flaps. A portion of fluid flow hits the partition wall, circulates and then exits from the side wall flaps. During this particular half cycle, 100% choking of the back-end rotor is ensured. This operational characteristic results in enhanced power output in comparison to the existing twin topology systems for fixed type OWC WECs as shown in Fig. 3.

Though there is a recirculation of flow between the trailing end of the front-end rotor and the partition wall still the flow exit from the rotor blades is not affected severely as depicted by Fig. 22(b).

The 3rd and the most crucial operational case of the proposed system was the flow through the front-end chamber during the exhalation cycle. For a more accurate and reliable result, this operational case was investigated using two sets of boundary conditions.

3D velocity streamlines for this case are shown in Fig. 24. The first set was with  $\Delta P_{OWC}$  as 0.5 atm below the atmosphere.  $\Delta P_{OWC}$  is the pressure drop in the phylum chamber due to the fall of OWC during the exhalation cycle. Fig. 24(a, b, c) presents the same.

It is evident that the fluid flow inlet is taking place from axial flap inlet and passing across front end rotor assembly and back into the phylum chamber. A small portion of fluid circulates before crossing the front-end rotor but it is not affecting the flow across the rotor assembly. An important observation here is that practically negligible flow exit is

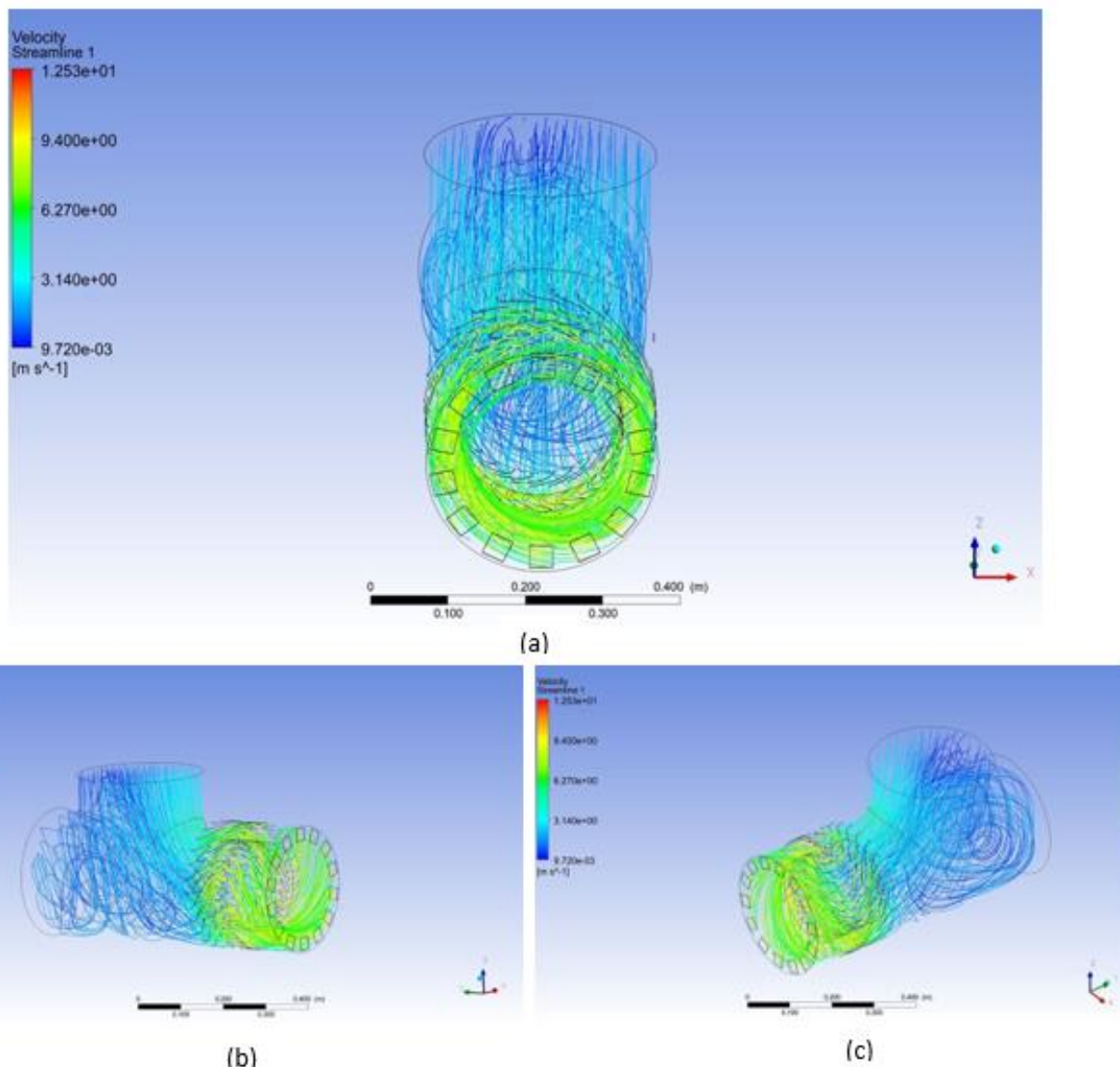


**Fig. 21:** 3D Velocity Streamlines: Back-end chamber (Exhalation)

taking place from side-wall flaps.

As the present work is focused upon low wave height conditions the fluid flow was reinvestigated with a lower  $\Delta P_{owc}$  as 0.25 atm below atmosphere. Fig. 24(d, e, f) presents the same. It is evident that here also practically negligible flow exit takes place from side wall flaps even at such a low pressure drop condition in phylum chamber. This validates the fact that side wall flaps will practically remain close during the exhalation half cycle. The adverse pressure of gradient between the axial flap inlet and phylum chamber prevents the flow exit from side wall flaps. This condition is exploited in the system and an additional power extraction is done from the front-end rotor during the exhalation cycle. During the second half cycle, instead of ensuring full choking of the front-end rotor it is run into operation. In the existing twin turbine topologies, the design motive is to utilize power from only one rotor at a time. But, in this proposed system, a hybrid scheme is followed to obtain maximum power output. During the exhalation cycle, primary momentum transfer from the fluid (air) to rotor takes place from the back-end rotor assembly. As, the air stream has to move back to front end chamber for exit, the air stream is again exploited for a secondary momentum transfer to the front-end rotor. Wave motion being a stochastic phenomenon, when the air stream will reach front end chamber from back-end chamber, the air inlet from suction inlet will also start to seize as result there is no case

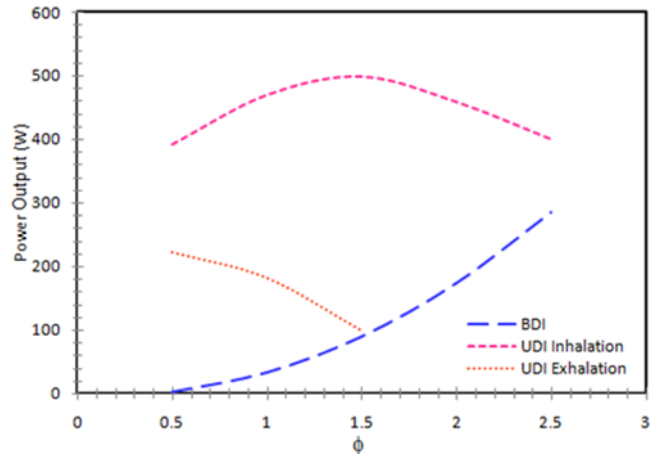


Fig. 23: Power output in different operational modes

interference between the operation of both the rotors during exhalation cycle. It can be commented that in low significant wave height and time period conditions, during operation of the front-end rotor, the back-end rotor will almost seize to operate.

As the front-end rotor operates without guide vanes and adverse placement of another set of guide vanes during exhalation cycle, it is expected that the power output will be reduced significantly. But, in the proposed system even this reduced power is an added advantage. The conventional BDI

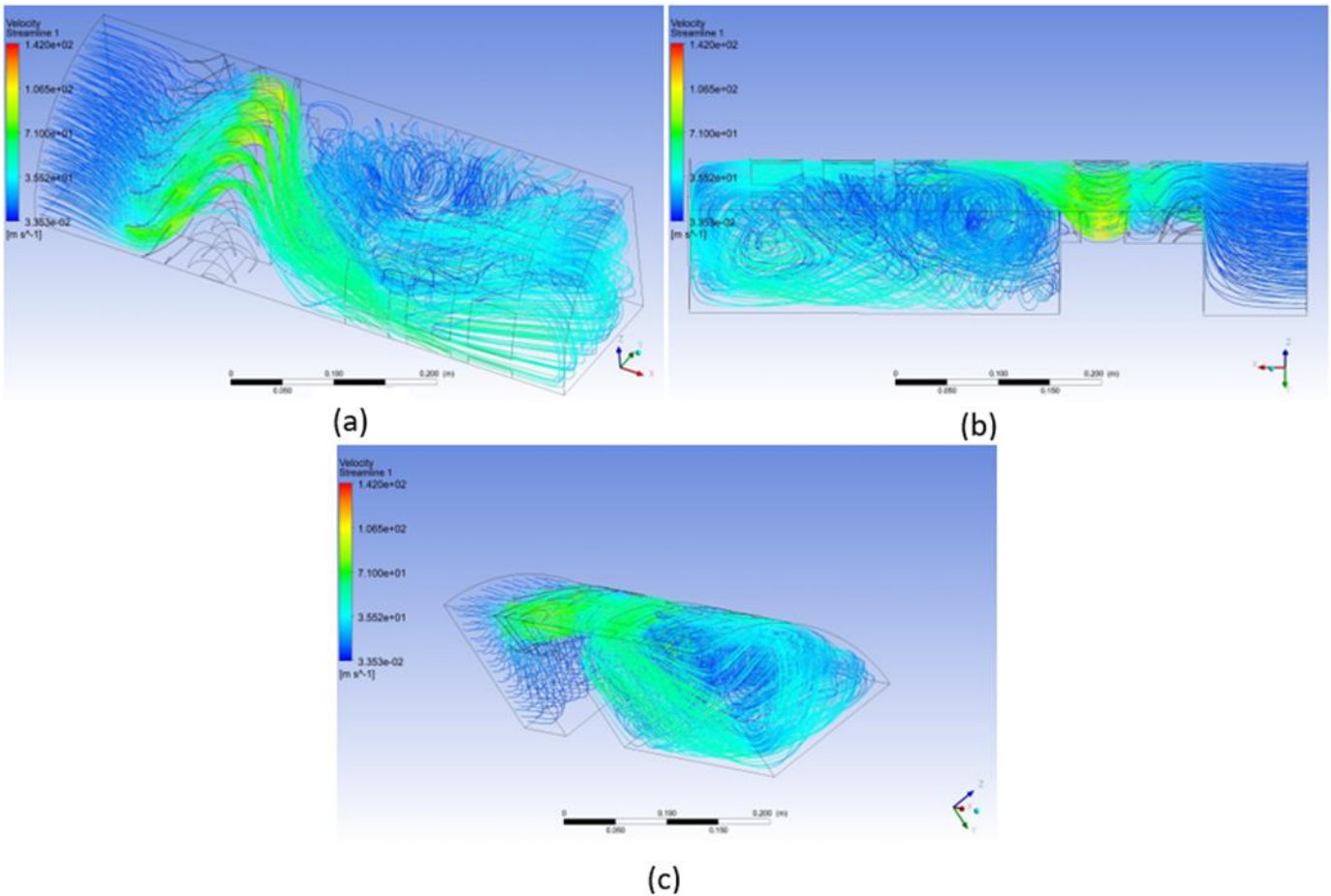


Fig. 22: 3D Velocity Streamlines: Front-end chamber (Inhalation)

and the proposed UDI turbine system was investigated under different operational cycles and power outputs were computed across a flow coefficient ranging from 0.5 to 2.

The power output from the system under different operational cycles is shown in Fig. 23. It is clearly evident that the UDI turbine produces considerably greater power output than the BDI turbine in both the operational cases i.e., inhalation and exhalation.

It is also evident that the UDI turbine under exhalation cycle stalls at  $\Phi = 1.5$ . It is probably due to absence of guide vane under Exhalation cycle along with adverse placement of guide vanes and under higher axial flow velocity, flow separation takes place at both leading and trailing edges. As

the present work is focused on low wave height conditions the system won't be operating at such higher flow coefficients.

The above inferences support the fact that the proposed flap based OWC WEC is operational under low wave height conditions. Following are the advantages which the proposed system will have under operation in comparison to the available OWC systems.

- As evident from Fig. 2, conventional OWC WEC employing UDI turbines consists of four types of flaps. The proposed flap-based system utilizes only two types of flaps which will result in operational simplicity and reduced maintenance expenses.

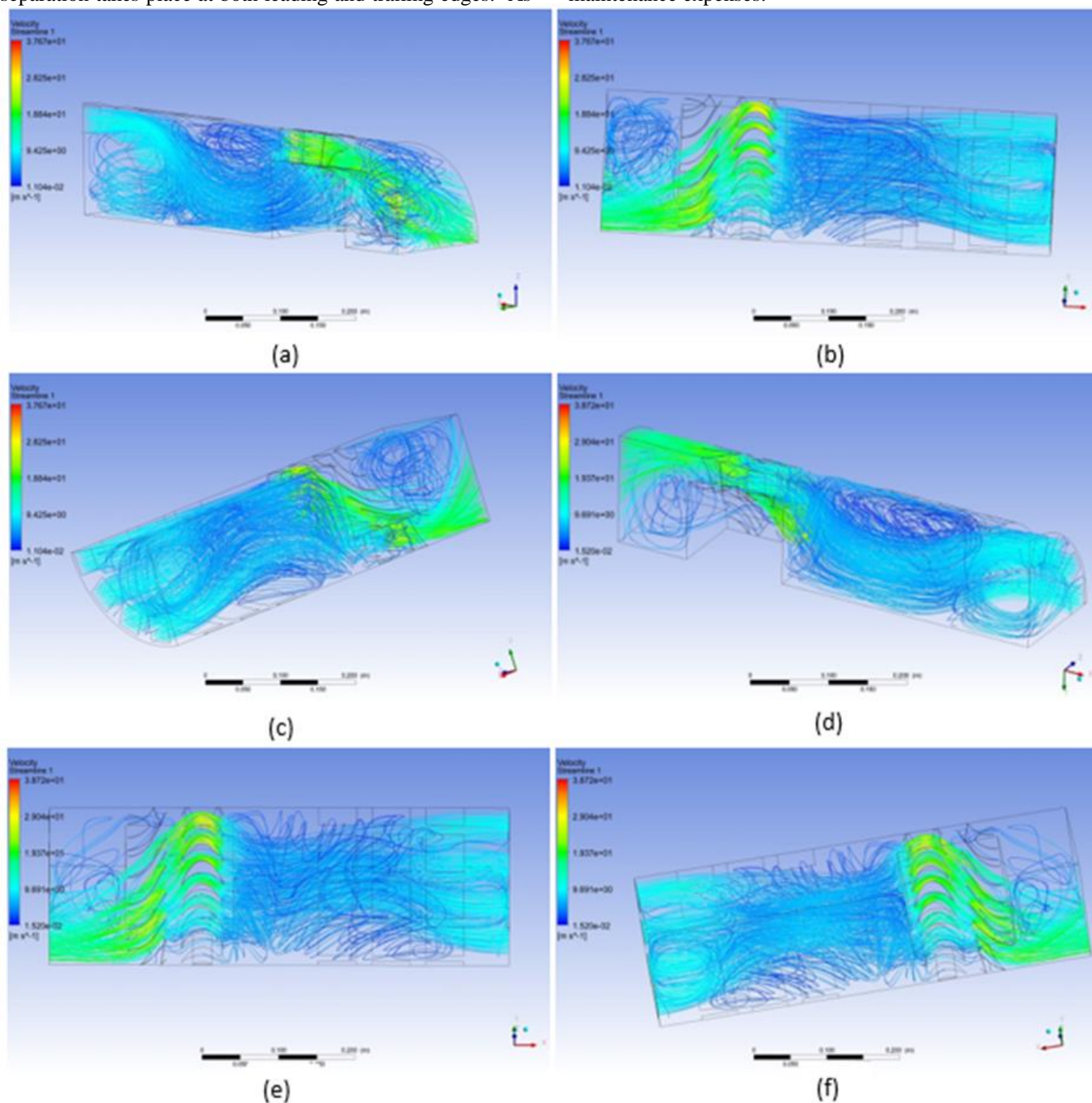


Fig. 24: 3D Velocity Streamlines: Front-end chamber (Exhalation)

- The twin-turbine topology explored by researchers till date assumes substantial choking of the idle turbine during reverse flow. But there is a limitation in the maximum choking possible even after the optimal design of guide vanes. The proposed system ensures practically full choking of the idle turbine during the inhalation cycle. Fig. 24 also portrays the fact that negligible flow leakage is occurring from sidewall flaps during the exhalation cycle.

- In the proposed system during the exhalation cycle, an additional energy extraction takes place even from the front-end rotor assembly during reverse flow. Such sort of provision was not available with the previously explored twin-turbine topologies. Fig. 23 supports the fact that the UDI turbine under reverse flow will provide considerable power output.

- Fig. 23 clearly enunciated the fact that under lower flow coefficients, a major increase in power output is produced under both inhalation and exhalation cycle. This particular observation clearly supports the fact that the proposed flap based OWC WEC is operationally viable under low wave height conditions.

## 6. Conclusion

In the present effort, a flap-based WEC was presented and compared to the conventional OWC WECs. The results of the numerical analysis clearly portray the fact that the proposed flap-based WEC converter employing dual rotors has enhanced power output in comparison to the conventional BDI and UDI turbine-based OWC WECs. It is observed that the proposed system works well under low wave height conditions. Along with enhanced power output, it is also observed that it has operational ease in comparison to conventional systems employing UDI turbines. An important inference from the present work is that UDI turbines (symmetric rotor blade profile with single guide vane on the upstream side) can also be employed for reverse flow under low wave height conditions. It is found that the proposed system works best in the vicinity of flow coefficient value of 1 and delivers maximum total power output. It was also found from the numerical study that the proposed system works well even with only two types of flaps in comparison to the conventional system where a minimum of four types of valves was necessary. Reduced variety of valves results in operational simplicity and lesser maintenance. The proposed hybrid scheme of full choking in the inhalation cycle and no choking in the exhalation cycle results in additional power output which is more than the primary power output of the conventional system in the flow coefficient range of 0.5 to 1.

## 7 Future Scope of Work

In the proposed system, the back-end rotor assembly is operational only under upstream flow and remains ideal under reverse flow. In this case, instead of using symmetric RB aerofoil, cambered aerofoil will result in enhanced powered output. A design of such RB aerofoil for low wave height conditions is essential. The authors are already working on numerical modeling of such an aerofoil.

Conventional OWC systems of this type work under rotational speed around 700 rpm. Authors believe that under low wave height conditions, a study of the relationship between inlet axial flow velocity and operational RPM is essential for best momentum transfer from the fluid to rotor blades. The authors are already done with the numerical simulation and the results will be presented in a forthcoming publication.

In the present study, it was found that there is a need for shape optimization of the back-end chamber near the trailing end such that even the minor losses due to recirculation can be minimized.

## Nomenclature

$X_{ss}$	Semi-major axis of ellipse (in mm)
$Y_{ss}$	Semi-minor axis of ellipse (in mm)
$R_{ps}$	Radius of circular arc of rotor blade pressure side (in mm)
$l_{rb}$	Chord length of rotor blade (in mm)
$R_{gv}$	Radius of Camber of Guide Vane (in mm)
$L_{gv}$	Length of straight line of Guide Vane (in mm)
$\rho_{rb}$	Radius of circular arc at the intersection of PS and SS (in mm)
$\theta$	Setting angle of guide vane (in °)
$\delta$	Camber angle of guide vane (in °)
$\lambda$	Rotor-stator axial distance (in mm)
$\rho_{gv}$	Radius of circular arc at guide vane edges (in mm)
$\sigma$	Guide Vane Thickness (in mm)
$v$	Spacing between circular and elliptical arc (in mm)
$\Delta P$	Pressure Difference across inlet and outlet (in Pa)
$Q$	Volume Flow Rate (in m <sup>3</sup> /s)
$\Delta P_{OWC}$	Pressure drop in phylum chamber due to fall of OWC during exhalation cycle (in atm)
$V_a$	Axial flow velocity (m/s)
$U$	Blade peripheral velocity (m/s)

## Abbreviation

atm	Atmospheric Pressure
BDI	Bi Directional Impulse
DGV	Downstream Guide Vane
OWC	Oscillating Water Column
OWEH	Ocean Wave Energy Harvesting
RANS	Reynolds Averaged Navier Stokes
RB	Rotor Blade
SST	Shear Stress Transport

UDI	Uni Directional Impulse
UGV	Upstream Guide Vane
WEC	Wave Energy Converter

## References

- [1] Y. Masuda, "An Experience of Wave Power Generator through Tests and Improvement," *Hydrodynamics of Ocean Wave-Energy Utilization*, pp. 445–452, 1986.
- [2] Y. Masuda, ME. McCormick, Experiences in pneumatic wave energy conversion in Japan. In: McCormick, ME, Kim, YC (eds) *Utilization of Ocean Waves—Wave to Energy Conversion*. New York: American Society of Civil Engineers, pp. 1–33, 1986.
- [3] A.A. Wells, Fluid Driven Rotary Transducer. (B.R. Patent No. 1,595,700), (1976).
- [4] I.A. Babinstev, Apparatus for Converting Sea Wave Energy into Electrical Energy. (U.S. Patent No. 3,922,739), (1975).
- [5] T. Setoguchi and M. Takao, "Current status of self-rectifying air turbines for wave energy conversion," *Energy Conversion and Management*, vol. 47, no. 15–16, pp. 2382–2396, Sep. 2006.
- [6] T. Setoguchi, K. Kaneko, H. Taryama, Maeda H, Inoue M. Impulse turbine with self-pitch-controlled guide vanes for wave power conversion: guide vanes corrected by links. *International Journal of Offshore and Polar Energy*;6(11), pp.76–88, 1996
- [7] H. MAEDA, T. SETOGUCHI, M. TAKAO, K. KANEKO, and M. INOUE, "Impulse Turbine with Air Flow Rectification System for Wave Power Conversion.," *TRANSACTIONS OF THE JAPAN SOCIETY OF MECHANICAL ENGINEERS Series B*, vol. 66, no. 646, pp. 1421–1427, 2000.
- [8] R. A. Arinaga and K. F. Cheung, "Atlas of global wave energy from 10 years of reanalysis and hindcast data," *Renewable Energy*, vol. 39, no. 1, pp. 49–64, Mar. 2012.
- [9] G. Saha, D. Majumdar, An overview study of Ocean energy potential and technologies in India. *Proceedings of 35th Indian Engineering Congress*, pp. 1229–1238, 2020
- [10] Y. Tominaga, M. Tanaka, H. Eto, Y. Mizuno, N. Matsui, and F. Kurokawa, "Design Optimization of Renewable Energy System Using EMO," 2018 International Conference on Smart Grid (icSmartGrid), Dec. 2018.
- [11] I. Guenoune, F. Plestan, and A. Chermitti, "Control of a new structure of twin wind turbine," 2016 IEEE International Conference on Renewable Energy Research and Applications (ICRERA), Nov. 2016.
- [12] M. Caruso, A. O. Di Tommaso, F. Genduso, R. Miceli, G. R. Galluzzo, C. Spataro, and F. Viola, "Experimental characterization of a wind generator prototype for sustainable small wind farms," 2016 IEEE International Conference on Renewable Energy Research and Applications (ICRERA), Nov. 2016.
- [13] K. D. Mercado, J. Jimenez, and M. C. G. Quintero, "Hybrid renewable energy system based on intelligent optimization techniques," 2016 IEEE International Conference on Renewable Energy Research and Applications (ICRERA), Nov. 2016.
- [14] M. Karimirad and K. Koushan, "WindWEC: Combining wind and wave energy inspired by hywind and wavestar," 2016 IEEE International Conference on Renewable Energy Research and Applications (ICRERA), Nov. 2016.
- [15] A. Harrouz, I. Colak, and K. Kayisli, "Control of a small wind turbine system application," 2016 IEEE International Conference on Renewable Energy Research and Applications (ICRERA), Nov. 2016.
- [16] T. K. Das, P. Halder, and A. Samad, "Optimal design of air turbines for oscillating water column wave energy systems: A review," *The International Journal of Ocean and Climate Systems*, vol. 8, no. 1, pp. 37–49, Feb. 2017.
- [17] M. Takao, Y. Kinoue, T. Setoguchi, T. Obayashi, and K. Kaneko, "Impulse Turbine with Self-pitch-controlled Guide Vanes for Wave Power Conversion (Effect of Guide Vane Geometry on the Performance)," *International Journal of Rotating Machinery*, vol. 6, no. 5, pp. 355–362, 2000.
- [18] A. George, B. Ranjith, A. Samad, and P. V. Dudhgaonkar, "Evaluation of Impulse Turbines for a Wave Energy Converter," Volume 1: Compressors, Fans and Pumps; Turbines; Heat Transfer; Combustion, Fuels and Emissions, Dec. 2017.
- [19] G. Maurya, T. K. Das, P. V. Dudhgaonkar, and A. Samad, "Effect of Guide Vane Fillets on Wave Energy Harvesting Impulse Turbine," Volume 1: Compressors, Fans, and Pumps; Turbines; Heat Transfer; Structures and Dynamics, Dec. 2019.
- [20] T. Karthikeyan, A. Samad, and R. Badhurshah, "Performance Enhancement of an Impulse Turbine Used for Ocean Energy Extraction," *Proceedings of the 5th International Congress on Computational Mechanics and Simulation*, 2014.
- [21] Y. Cui and Z. Liu, "Effects of Solidity Ratio on Performance of OWC Impulse Turbine," *Advances in Mechanical Engineering*, vol. 7, no. 1, p. 121373, Dec. 2014.
- [22] A. Thakker, M. Takao, T. Setoguchi, and T. S. Dhanasekaran, "Effects of Compressibility on the Performance of a Wave-Energy Conversion Device with an Impulse Turbine Using a Numerical Simulation Technique," *The International Journal of Rotating Machinery*, vol. 9, no. 6, pp. 443–450, Nov. 2003.
- [23] R. Badhurshah and A. Samad, "Surrogate Assisted Design Optimization of an Air Turbine," *International Journal of Rotating Machinery*, vol. 2014, pp. 1–8, 2014.
- [24] H. Maeda, S. Santhakumar, T. Setoguchi, M. Takao, Y. Kinoue, and K. Kaneko, "Performance of an impulse turbine with fixed guide vanes for wave power conversion," *Renewable Energy*, vol. 17, no. 4, pp. 533–547, Aug. 1999.
- [25] K. Ezhilsabareesh, R. Suchithra, and A. Samad,

“Performance enhancement of an impulse turbine for OWC using grouped grey wolf optimizer-based controller,” *Ocean Engineering*, vol. 190, p. 106425, Oct. 2019.

[26] T. Setoguchi, M. Takao, S. Santhakumar, and K. Kaneko, “Study of an Impulse Turbine for Wave Power Conversion: Effects of Reynolds Number and Hub-to-Tip Ratio on Performance,” *Journal of Offshore Mechanics and Arctic Engineering*, vol. 126, no. 2, pp. 137–140, May 2004.

[27] M. Takao and T. Setoguchi, “Air Turbines for Wave Energy Conversion,” *International Journal of Rotating Machinery*, vol. 2012, pp. 1–10, 2012.

[28] A. Thakker, P. Frawley, H.B. Khaleeq, Y. Abugihalia, and T. Setoguchi. "Experimental And CFD Analysis of 0.6m Impulse Turbine with Fixed Guide Vanes." Paper presented at the The Eleventh International Offshore and Polar Engineering Conference, Stavanger, Norway, June 2001.

[29] R. Badhurshah, A. Samad, and J. Sangwai, “Analysis of Flow through Ocean Energy Harvesting Bidirectional Impulse Turbine,” *The International Journal of Ocean and Climate Systems*, vol. 5, no. 2, pp. 51–63, Jun. 2014.

[30] R. Badhurshah, P. Dudhgaonkar, P. Jalihal, and A. Samad, “High efficiency design of an impulse turbine used in oscillating water column to harvest wave energy,” *Renewable Energy*, vol. 121, pp. 344–354, Jun. 2018.

[31] C. Xiong and Z. Liu, “Numerical Analysis on Impulse Turbine for OWC Wave Energy Conversion,” 2011 Asia-Pacific Power and Energy Engineering Conference, Mar. 2011.

[32] Z. Liu, J. Jin, Y. Cui, and H. Fan, “Numerical Analysis of Impulse Turbine for Isolated Pilot OWC System,” *Advances in Mechanical Engineering*, vol. 5, p. 416109, Jan. 2013.

[33] R. P. F. Gomes, J. C. C. Henriques, L. M. C. Gato, and A. F. O. Falcão, “Multi-point aerodynamic optimization of the rotor blade sections of an axial-flow impulse air turbine for wave energy conversion,” *Energy*, vol. 45, no. 1, pp. 570–580, Sep. 2012.

[34] A. Thakker, Frawley, Patrick, H. Khaleeq, Y. Abugihalia, T. Setoguchi, Experimental and CFD Analysis of 0.6m Impulse Turbine with Fixed Guide Vanes, 2001

[35] V. Jayashankar, S. Anand, T. Geetha, S. Santhakumar, V. Jagadeesh Kumar, M. Ravindran, T. Setoguchi, M. Takao, K. Toyota, and S. Nagata, “A twin unidirectional impulse turbine topology for OWC based wave energy plants,” *Renewable Energy*, vol. 34, no. 3, pp. 692–698, Mar. 2009.

[36] S. Okuhara, M. Takao, H. Sato, A. Takami, and T. Setoguchi, “A Twin Unidirectional Impulse Turbine for Wave Energy Conversion—Effect of Fluidic Diode on the Performance,” *Open Journal of Fluid Dynamics*, vol. 04, no. 05, pp. 433–439, 2014.

[37] ANSYS Fluent User’s Guide 12.0 Section 10.3.1

[38] S. M., Yahya, *Turbines, Compressors and fans*, Tata McGraw-Hill Education, New Delhi, 2013